

# HUBBLE SPACE TELESCOPE IDENTIFICATION OF THE OPTICAL COUNTERPARTS OF ULTRALUMINOUS X-RAY SOURCES IN M51

YUICHI TERASHIMA<sup>1</sup>, HIROHIKO INOUE<sup>1,2</sup>, AND ANDREW S. WILSON<sup>3,4</sup>  
*To appear in The Astrophysical Journal.*

## ABSTRACT

We present the results of a search for optical identifications of ultraluminous X-ray sources (ULXs) in M51 by using mosaic images taken with the *Hubble Space Telescope* Advanced Camera for Surveys in filters F435W (B), F555W (V), F814W (I), and F658N (H $\alpha$ ). Our sample consisting of nine ULXs is defined by analyzing the three *Chandra* observations of M51 performed in 2000 June, 2001 June, and 2003 Aug. We found four ULXs have one or two candidates for counterparts, while two have multiple stars within their error circles. The other three have no candidate counterparts. Four ULXs are located near or in a star cluster, while others have no association with a cluster. These results indicate that the companion star, environment, and origin of ULXs are probably heterogeneous.

*Subject headings:* X-rays: binaries — X-rays: galaxies — X-rays: stars — galaxies: Individual (M51)

## 1. INTRODUCTION

A fraction of galaxies contain X-ray sources whose luminosities exceed  $10^{39}$  erg s<sup>-1</sup>; these sources are known as ultraluminous compact X-ray sources (ULXs; Makishima et al. 2000). Their nature is still under debate, with models including a black hole with a mass greater than a few times  $10M_{\odot}$  (intermediate mass black hole; IMBH), super Eddington accretion or beamed emission from a neutron star or stellar mass black hole (e.g., Miller & Colbert 2004; Fabbiano & White 2005). Optical counterparts of ULXs have the potential to provide us with significant insights into the nature of ULXs. If a companion star is detected, it could be used to measure the mass function of a ULX binary system. The environments of ULXs are also quite useful for elucidating the origin and formation mechanism of ULXs.

Optical counterparts of ULXs have been searched for from the ground and with the *Hubble Space Telescope* (*HST*). One or a few O–B type stars have been proposed as candidates for the companion star of some ULXs (e.g., M81, Liu et al. 2002; NGC 5204, Liu et al. 2004; M101 Kuntz et al. 2005), while some ULXs have no obvious stellar counterparts (e.g., NGC 4559 X10, Cropper et al. 2004). Many ULXs are located near a star cluster (e.g., Kaaret et al. 2004), or the center of an optical emission line nebula, which may be a supernova remnant or ionized by hot stars (e.g., Pakull & Mirioni 2002; Liu et al. 2005; see Liu & Mirabel 2005 for a catalog). These environments are suggestive of an episode of recent star formation and a close connection between the formation of ULXs and stars. Some ULXs reside in a high-excitation optical emission-line nebula that may be photoionized by unbeamed X-ray emission from one or more of the ULXs (Pakull & Mirioni 2002). Thus the optical counterparts and environments of ULXs are not uniform and might suggest a heterogeneous nature for ULXs. Therefore, more systematic searches for ULX counterparts are of great importance.

M51 (NGC 5194 and its companion NGC 5195) is an ideal object in which to search for optical counterparts and to investigate their environments in a systematic way because of its large

number of ULXs (seven in NGC 5194 and two in NGC 5195; Terashima & Wilson 2004) and relative proximity (8.4 Mpc; Feldmeier et al. 1997). The X-ray luminosities of the ULXs are modest and in a narrow range ( $1-4 \times 10^{39}$  erg s<sup>-1</sup>). These facts make the M51 ULXs valuable for studying ULXs with luminosities between ordinary black holes ( $< 10^{39}$  erg s<sup>-1</sup>) and their highest known values ( $\sim 10^{41}$  erg s<sup>-1</sup>; M82, Matsumoto et al. 2001; NGC 2276 Davis & Mushotzky 2004). Liu et al. (2005) imaged two ULXs (CXOM51 J133001.0+471344 and CXOM51 J133007.6+471106) with *HST* WFPC2 in filters F450W, F555W, and F814W. The former ULX is located on the rim of a star cluster and there exist a few faint stars in the error circle, while there are seven stellar objects within the error circle of the latter. There are no bright stars younger than 10 million years in the error circles. Liu et al. (2005) estimated that these two ULXs are in regions with stars younger than  $10^{7.8}$  years.

In this paper, we present candidates for optical counterparts and environments of all of the nine ULXs in M51 by utilizing the fine spatial resolution and wide field of view of a recent observation with the *HST* Advanced Camera for Surveys (ACS).

## 2. OBSERVATIONS AND ANALYSIS

### 2.1. *Chandra* Observations

A sample of ULXs in M51 was constructed by analyzing three *Chandra* data sets obtained on 2000 June 20, 2001 June 23–24, and 2003 August 7–8, with effective exposure times of 14.9, 26.8, and 42.9 ksec, respectively. Results from the first and second observations are presented in Terashima & Wilson (2004), while we have newly analyzed the last data obtained by us. Using the first two data sets, Terashima & Wilson (2004) found nine ULXs, defined as off-nuclear X-ray sources each with a luminosity greater than  $10^{39}$  erg s<sup>-1</sup> in the 0.5–8 keV band. These nine ULXs are shown in Table 1. The names for the ULXs are also defined in Table 1 in order of increasing right ascension. Liu & Mirabel (2005) assigned the same numbers from ULX-1 to ULX-7. Liu et al. (2005) used different defi-

<sup>1</sup> Institute of Space and Astronautical Science, 3-1-1 Yoshinodai, Sagami-hara, Kanagawa 229-8510, Japan

<sup>2</sup> Department of Physics, Tokyo Institute of Technology, 2-12-1, Ohokayama, Meguro, Tokyo 152-8551, Japan

<sup>3</sup> Astronomy Department, University of Maryland, College Park, MD 20742

<sup>4</sup> Adjunct Astronomer, Space Telescope Science Institute, 3700 San Martin Drive, Baltimore, MD 21218

nitions: their ULX-3 and ULX-5 are our ULX-7 and ULX-9, respectively.

The three *Chandra* observations were combined to perform an X-ray source search with the best available photon statistics. Source detection was performed by using “wavdetect” in the CIAO version 3.0.2 software package. Details of the procedures are the same as in Terashima & Wilson (2004). The resulting source list was compared with source positions obtained in other wavebands. One optical/near infrared star and the radio nucleus of NGC 5194 were used to estimate the accuracy of astrometry and we found their source positions agree to within  $\approx 0.2$  arcsec with the *Chandra* X-ray positions (the near infrared position of the star was taken from the 2MASS catalog, while the radio position of the nucleus was taken from a VLA observation in A-configuration (Hagiwara et al. 2001). Since the directions of the offsets of source positions were not systematic, we made no corrections to the coordinates. The newly-determined positions of the ULXs are shown in Table 1. The new positions are in good agreement with the previous measurement, and differences are typically 0.1 arcsec or less. The statistical errors of the positions of the ULXs are 0.07 arcsec or better.

## 2.2. HST Observations

The M51 system was mapped with the *HST* ACS in 2005 Jan. as a part of the Hubble Heritage program. The data consist of six ( $2 \times 3$ ) images in the four filters F435W (B), F555W (V), F814W (I), and F658N ( $H\alpha$ ), with exposure times of 2720, 1360, 1360, and 2720 sec, respectively. We use the drizzle-combined fits images (the version 1.0 mosaics) taken from the archives in the following analysis. We measured the positions and fluxes of detected sources by point-spread function fitting to the images using the *daophot* package.

In order to improve the astrometry of the *HST*, we compared point-like sources in the ACS images with sources listed in the 2MASS catalogue and found systematic offsets of 0.1 arcsec and 0.7 arcsec in the right ascension and declination directions, respectively. We shifted the ACS images to the 2MASS positions. After this alignment, we searched for coincident point-like sources detected in both the ACS and *Chandra* images. Four X-ray sources (CXOM51 J132938.6+471336, CXOM51 J132938.9+471324, CXOM51 J132943.4+471525, and CXOM51 J133011.0+471041) have point-like counterparts in the ACS images. All four sources are detected in the three bands B, V, and I. These sources are relatively bright in X-rays and have 130–310 counts in the 0.5–8 keV band in the combined data of the three observations. The statistical errors of their *Chandra* positions are 0.05–0.12 arcsec. The rms of the position differences between *Chandra* and *HST* are 0.09 and 0.10 arcsec in the directions of right ascension and declination, respectively. Thus, we adopt 0.1 arcsec as the uncertainty between the source locations in the optical and X-ray images. We use a one sigma uncertainty of 0.14 arcsec by combining both this uncertainty (0.1 arcsec) and the X-ray position error of the ULXs (better than 0.1 arcsec) in quadrature. If we assume the probability distribution of a source location is a 2-dimensional Gaussian, this uncertainty corresponds to a 90% confidence error radius of 0.3 arcsec (12 pc), which is used throughout this paper.

## 3. RESULTS

### 3.1. X-ray Spectra and Variability

Among the nine ULXs found in the observations in 2000 and 2001, only four (ULX-2, 3, 7, and 9) fulfil the definition of a ULX in the data obtained in 2003. The luminosities of three other ULXs (ULX-1, 5, and 8) decreased to  $(7-9) \times 10^{38}$  erg  $s^{-1}$  and two objects (ULX-4 and ULX-6) diminished to below  $1.0 \times 10^{37}$  and  $9.2 \times 10^{36}$  erg  $s^{-1}$  in the 0.5–8 keV band (95% confidence upper limit), respectively, where we assumed a power law spectrum with a photon index of 2.0 modified by the Galactic absorption ( $N_H = 1.4 \times 10^{20}$  cm $^{-2}$ ). No new ULXs appeared in the 2003 observation. It is interesting to note that the two objects ULX-4 and ULX-6 were detected only in the 2001 observation and that their spectra are completely different: a power law with a photon index of 1.55 and an MCD with an inner disk temperature of 0.10 keV.

We modelled the X-ray spectra of the seven sources detected in 2003 using the XSPEC spectral fitting package. The spectra were grouped so that each spectral bin contained at least 20 counts to allow use of the  $\chi^2$  minimization technique. Background spectra were taken from a source-free region near the source and subtracted from the on-source spectra. Two continuum models, a power law and a multicolor disk blackbody (MCD; Mitsuda et al. 1984) modified by photoelectric absorption, were examined. The results of spectral fitting for the third *Chandra* observation (in 2003) are summarized in Table 2, while the results for the 2000 and 2001 observations are presented in Terashima & Wilson (2004). The observed fluxes and absorption corrected luminosities are also shown. The spectra of three ULXs (ULX-5, 7, and 9) are better fitted with a power law than an MCD model. ULX-2 shows a very soft spectrum and an MCD fits the data better. We applied a blackbody model to the spectrum of ULX-2 and obtained a similar quality of fit. The result is also shown in Table 2. Other ULXs are well fitted with either a power law or an MCD model.

We examined the light curves of the seven ULXs detected in all three observations. ULX-1, 2, 7, and 8 showed mild variability. Their intensities changed by a factor of 1.5–2 in several thousand to ten thousand seconds. A two hour periodicity in ULX-7 reported in Liu et al. (2002) was not confirmed. Only two (or maybe three) periods are seen at the beginning of the observation, but the periodicity is not clear in the latter half.

### 3.2. Optical Counterparts

Fig. 1 shows a true-color image around the nine ULXs. There are one or two candidate stellar counterparts in the error circles of ULX-1, 2, 8, and 9. The apparent magnitudes of these stars are shown in Table 3. A very faint star may be present as well within the error circles of ULX-1 and ULX-2. There are no dense or large star clusters near ULX-1, but ULX-1 may be in a shell with an oval shape seen in an  $H\alpha$  image (Fig. 2). The diameter of the structure is about 260 pc. The  $H\alpha$  luminosity of this structure is  $4.9 \times 10^{36}$  erg  $s^{-1}$ , which includes red-shifted [N II] $\lambda$ 6583 located in the filter bandpass. ULX-2 is located near the rim of a large star cluster. The projected distance between ULX-2 and the center of this cluster is about 170 pc. ULX-8 is in the tidal tail connecting NGC 5194 and NGC 5195 and located 2.8 kpc east of the nucleus of NGC 5195. There are two very faint sources in the error circle in the B band image. No  $H\alpha$  emitting region is seen around this ULX. There is one source in the error circle of ULX-9. This counterpart corresponds to “c1” presented in Liu et al. (2005). ULX-9 seems not to be associated with a cluster: the projected distance to the nearest cluster is 240 pc. It is worth noting that this distance

is larger than a trend suggested by observations that X-ray binaries with a higher luminosity tend to be located near a star cluster (Kaaret et al. 2004). Images of the  $2.5'' \times 2.5''$  region around the ULXs with possible counterparts are shown in Fig. 3.

We measured the apparent magnitude and colors of the candidate IDs in the STMAG system. Results are summarized in Table 3. The amount of the Galactic extinction derived from H I maps is negligible ( $A_V \approx 0$ ; Burstein & Heiles 1984) and no correction was made. These magnitudes are converted to the Johnson system by referring to Sirianni et al. (2005), and color-magnitude diagrams are plotted in Fig. 4 along with the evolutionary tracks with  $Z = 0.02$  of Lejeune & Schaerer (2001).  $Z = 0.02$  corresponds to the solar metallicity  $[\text{Fe}/\text{H}] = 0$ . The magnitude and colors of the candidate counterparts of ULX-1, ULX-2, and ULX-9 are consistent with B2-8, O5-B2, and F2-5 supergiants, respectively. The B-band magnitudes of the two candidate counterparts to ULX-8 are consistent with B2V type.

The colors of the candidate IDs were compared with those of quasars to test whether the optical sources are consistent with background AGNs. We used 38349 quasars at a redshift  $z < 2.1$  in the Sloan digital sky survey third data release (Schneider et al. 2005). Photometric data taken at the  $g$ ,  $r$ , and  $i$  bands were converted to the colors  $B-V$  and  $V-I$  by using the conversion factors appropriate for  $z < 2.1$  given in Table 1 of Jester et al. (2005). None of the quasars have colors consistent with the candidate counterparts of ULX-1 and ULX-2, while the color of the ULX-9 counterpart is in the range of the quasars. The expected number of background AGNs with a flux in the 0.5–8 keV band greater than  $1.2 \times 10^{-13}$  erg  $\text{s}^{-1} \text{cm}^{-2}$  (i.e.,  $1.0 \times 10^{39}$  erg  $\text{s}^{-1}$  at 8.4 Mpc) coincidentally detected within the areas of NGC 5194 and NGC 5195 is 0.24 and 0.021, respectively, if the  $\log N$ - $\log S$  relation in the 2–10 keV band shown in Fig. 3 of Ueda et al. (2003) and a photon index of 1.8 are assumed.

We estimated the probability that these counterparts are chance coincidences with an unrelated star. An error circle with a radius of 0.3 arcsec was randomly placed in the region around the ULXs and we calculated the probability of detection of one or more stars within the circle. Since the probabilities are a function of the magnitude of the stars, the following two cases were examined: detection of stars of any brightness detected in the ACS observation and of brightness greater than or equal to that of the proposed ID. The results are shown in Table 3.

The two ULXs ULX-4 and ULX-7 are in a region with a relatively high stellar density in or near a star cluster. ULX-4 is located near the center of a star cluster, and there are many stars within the error circle. ULX-7 is near the rim of a cluster and there are at least four stars in the error circle.

There are no obvious optical counterparts for ULX-3, 5, and 6. ULX-3 is located at the position of one of the dark lanes in the inner spiral arms. Its large X-ray absorbing column density,  $N_{\text{H}} \approx 5 \times 10^{22}$   $\text{cm}^{-2}$  (Terashima & Wilson 2004), is qualitatively consistent with the location. Thus, extinction to this object is likely to be large, and our data cannot rule out the presence of optically luminous counterparts. A hint of the presence of a very faint star may be a counterpart suffering from heavy extinction. This region is bright in  $\text{H}\alpha$ . ULX-5 is located outside the outer arm. The stellar density around there

is relatively small and there are no bright stars. An extended source visible in all the optical bands is present 80 pc west of ULX-5. An  $\text{H}\alpha$  image of the extended source consists of a ring-shaped structure with a radius of about 50 pc and a bright spot at around (13:29:53.55, +47:14:35.6) (J2000.0). It is not clear whether this object is related to the ULX or not. ULX-6 is in the bright stellar envelope of NGC 5195. Individual point sources are not clearly seen in this region. In summary, there is no clear association with a star or star cluster for ULX-3, 5 or 6.

Association with a star cluster is of significant importance for understanding the environment of ULXs. Among the nine ULXs, four (ULX-2, 4, 7, and 9) are located near the center or rim of a star cluster. Their  $\text{H}\alpha$  images show diffuse emission surrounding the clusters. These ULXs are located around the rim of the extended emission.

#### 4. DISCUSSION

The ACS images show that the ULXs in M51 can be classified into three subclasses in terms of their optical counterparts: (1) there are one or two stars in the error circle, (2) the ULX is located in a region with relatively high stellar density and multiple candidate counterparts are present, and (3) there are no candidate counterparts.

The spectral types of the candidate companion stars of ULX-1 and ULX-2 are as early as OB-type and indicate that these systems are high-mass X-ray binaries. Candidate companions of such early type stars are also reported for ULXs in other galaxies. The counterpart of ULX-9 has a later spectral type (F-type). A comparison with the isochrones for  $Z=0.02$  (Lejeune & Schaerer 2001) shows that the counterparts of ULX-1 and ULX-2 have an age of  $10^{6.6-7.2}$  yrs, while that of the counterpart of ULX-9 is around  $10^{7.6-7.8}$  yrs. Some other ULXs also have lower mass companions; a main sequence star with the limiting magnitude of these observation ( $M_B = 0.4$ ) or fainter corresponds to A- or later type. Thus, there exist both high-mass and low-mass companions among the ULXs in M51.

The ULXs in our sample are in two environments: (1) ULXs located in or near a star cluster or associated with an H II region, and (2) no connection to a star cluster. This fact suggests that the presence of a star cluster is not always required to form a ULX. If ULXs not associated with a star cluster do contain an IMBH, IMBH could be formed by a process independent of recent star formation or a star cluster currently observed. In this case, an IMBH may be a remnant of past active star formation or a population III star (Madau & Rees 2001). Alternatively, the compact object in ULXs could have a stellar mass expected from the known evolution of ordinary stars. If this is the case, the observed X-ray luminosities require only mild (a factor of a few) super-Eddington luminosities for a  $10M_{\odot}$  black hole, for example. Such a luminosity is expected by some workers from an accretion disk with a high accretion rate (e.g., Ohsuga et al. 2003). Thus the wide variety of the environments may suggest a heterogeneous ULX formation history and/or black hole mass at least for ULXs with a moderate luminosity (a few  $\times 10^{39}$  erg  $\text{s}^{-1}$ ).

This research was partially supported by NASA through LTSA grant NAG 513065 to the University of Maryland.

## REFERENCES

- Burstein, D., & Heiles, C. 1984, *ApJS*, 54, 33
- Cropper, M., Soria, R., Mushotzky, R. F., Wu, K., Markwardt, C. B., & Pakull, M. 2004, *MNRAS*, 349, 39
- Davis, D. S., & Mushotzky, R. F. 2004, *ApJ*, 604, 653
- Feldmeier, J. J., Puls, J., & Pauldrach, A. W. A. 1997, *ApJ*, 479, 231
- Fabbiano, G., & White, N. E. 2005, in "Compact Stellar X-ray Sources" ed. W. Lewin & M. van der Klis (Cambridge: Cambridge University Press), in press
- Hagiwara, Y., Henkel, C., Mentem, K. M., & Nakai, N. 2001, *ApJ*, 560, 119
- Jester, S., et al. 2005, *AJ*, 130, 873
- Kaaret, P., Alonso-Herrero, A., Gallagher, III, J. S., Fabbiano, G., Zezas, A., & Rieke, M. J. 2004, *MNRAS*, 348, L28
- Kuntz, K. D., Gruendl, R. A., Chu, Y.-H., Chen, C.-H. R., Still, M., Mukai, K., & Mushotzky, R. F. 2005, *ApJ*, 620, L31
- Lejeune, T., & Schaerer, D. 2001, *A&A*, 366, 538
- Liu, J.-F., Bregman, J. N., & Seitzer, P. 2002, *ApJ*, 580, L31
- 2004, *ApJ*, 602, 249
- Liu, J.-F., Bregman, J. N., Seitzer, P., & Irwin, J. 2005, *AJ*, submitted (astro-ph/0501310)
- Liu, Q. Z., & Mirabel, I. F. 2005, *A&A*, 429, 1125
- Madau, P., & Rees, M. J. 2001, *ApJ*, 551, L27
- Makishima, K., et al. 2000, *ApJ*, 535, 632
- Matsumoto, H., et al. 2001, *ApJ*, 547, L25
- Miller, M. C., & Colbert, E. J. M. 2004, *Int. J. Mod. Phys. D*, 13, 1
- Mitsuda, K., et al. 1984, *PASJ*, 36, 741
- Ohsuga, K., Mineshige, S., & Watarai, K. 2003, *ApJ*, 596, 429
- Pakull, M. W., & Mirioni, L. 2002, in "New Visions of the X-ray Universe in the XMM-Newton and Chandra Era", ed. F. Jansen et al. (ESA SP 488; Noordwijk: ESA) (astro-ph/0202488)
- Schneider, D. P., et al. 2005, *AJ*, 130, 367
- Sirianni, M., et al. 2005, *PASP*, 117, 1049
- Ueda, Y., Akiyama, M., Ohta, K., & Miyaji, T. 2003, *ApJ*, 598, 886
- Terashima, Y., & Wilson, A. S. 2004, *ApJ*, 601, 735

TABLE 1  
ULTRALUMINOUS COMPACT X-RAY SOURCES IN M51

ULX Number	CXO Name <sup>a</sup> CXOM51	X-ray Position <sup>b</sup>	
		R.A. (J2000.0)	Dec. (J2000.0)
ULX-1	J132939.5+471244	13 29 39.47	+47 12 43.60
ULX-2	J132943.3+471135	13 29 43.31	+47 11 34.80
ULX-3	J132950.7+471155	13 29 50.68	+47 11 55.21
ULX-4	J132953.3+471042	13 29 53.31	+47 10 42.46
ULX-5	J132953.7+471436	13 29 53.72	+47 14 35.74
ULX-6	J132958.4+471547	13 29 58.38	+47 15 47.40
ULX-7	J133001.0+471344	13 30 01.01	+47 13 43.93
ULX-8	J133006.0+471542	13 30 06.00	+47 15 42.30
ULX-9	J133007.6+471106	13 30 07.55	+47 11 06.11

Note. — *a*: *Chandra* name presented in Terashima & Wilson (2004). *b*: X-ray positions newly determined in this paper.

TABLE 2  
X-RAY SPECTRAL PARAMETERS

ULX Name	$N_{\text{H}}$ ( $10^{22} \text{ cm}^{-2}$ )	Photon index	$kT_{\text{in}}$ (keV)	Flux <sup>a</sup> ( $10^{-14} \text{ erg s}^{-1} \text{ cm}^{-2}$ )	Luminosity <sup>b</sup> ( $10^{39} \text{ erg s}^{-1}$ )	$\chi^2/\text{dof}$
ULX-1	$0.18^{+0.07}_{-0.08}$ $0.027^{+0.053}_{-0.027}$	$1.99^{+0.29}_{-0.22}$ ...	...	6.5	0.70	16.1/15
ULX-2	$0.58^{+0.12}_{-0.15}$ $0.50^{+0.16}_{-0.17}$	... ...	$1.09^{+0.28}_{-0.22}$ $0.092 \pm 0.003$	5.6 3.7	0.49 9.7	17.8/15 29.9/28
ULX-3	$3.8^{+1.1}_{-1.0}$ $3.1 \pm 0.7$	$1.52^{+0.54}_{-0.41}$ ...	... $2.9^{+2.2}_{-0.9}$	19.0 18.6	3.3 2.5	48.0/37 49.1/37
ULX-4	$0.014^d$	$2.0^d$	..	$< 0.12^e$	$< 0.010^e$	...
ULX-5	$0.19^{+0.03}_{-0.06}$ 0.050	$1.73^{+0.13}_{-0.17}$ ...	... 1.4	8.5 ...	0.79 ...	25.2/22 34.3/22
ULX-6	$0.014^d$	$2.0^d$	...	$< 0.11^e$	$< 0.0092^e$	...
ULX-7	$0.16^{+0.04}_{-0.03}$ $0.049^{+0.021}_{-0.018}$	$1.49^{+0.13}_{-0.12}$ ...	... $1.86^{+0.27}_{-0.23}$	32.7 30.3	3.2 2.7	42.3/49 60.9/49
ULX-8	$0.15^{+0.05}_{-0.06}$ $0.022^{+0.042}_{-0.022}$	$1.76^{+0.13}_{-0.19}$ ...	... $1.34^{+0.36}_{-0.27}$	7.1 6.2	0.71 0.53	8.4/18 11.9/18
ULX-9	$0.25 \pm 0.03$ 0.075	$2.26 \pm 0.13$ ...	... 0.97	24 ...	3.0 ...	79.2/54 118.3/54

Note. — *a*: Observed flux in the 0.5–8 keV band. *b*: Luminosity corrected for absorption in the 0.5–8 keV band. *c*: Blackbody model fit. *d*: Assumed parameters. *e*: 95% confidence upper limit.

TABLE 3  
OPTICAL POSITIONS AND MAGNITUDE

Name	Optical Position		Magnitude <sup>a</sup>			Chance probability <sup>b</sup>
	R.A. (J2000.0)	Dec. (J2000.0)	B	V	I	
ULX-1	13 29 39.467	+47 12 43.55	22.59	23.27	24.80	0.004 (0.48)
ULX-2	13 29 43.309	+47 11 34.73	23.20	24.01	25.50	0.17 (0.79)
ULX-8	13 30 06.001	+47 15 42.28	26.51	...	...	0.29 (0.29)
	13 30 05.977	+47 15 42.12	26.03	...	...	...
ULX-9	13 30 07.547	+47 11 06.07	25.17	25.49	26.04	0.27 (0.47)

Note. — (a) Magnitude in the STMAG system, defined as  $-2.5 \times \log_{10} F - 21.10$ , where  $F$  is a measured flux in units of  $\text{erg cm}^{-2} \text{s}^{-1} \text{A}^{-1}$ . (b) Probability that an unrelated star is detected in the error circle. Probabilities are for stars of brightness greater than or equal to that of the proposed ID. Probabilities for stars of any brightness detected by the ACS observation are shown in parentheses.

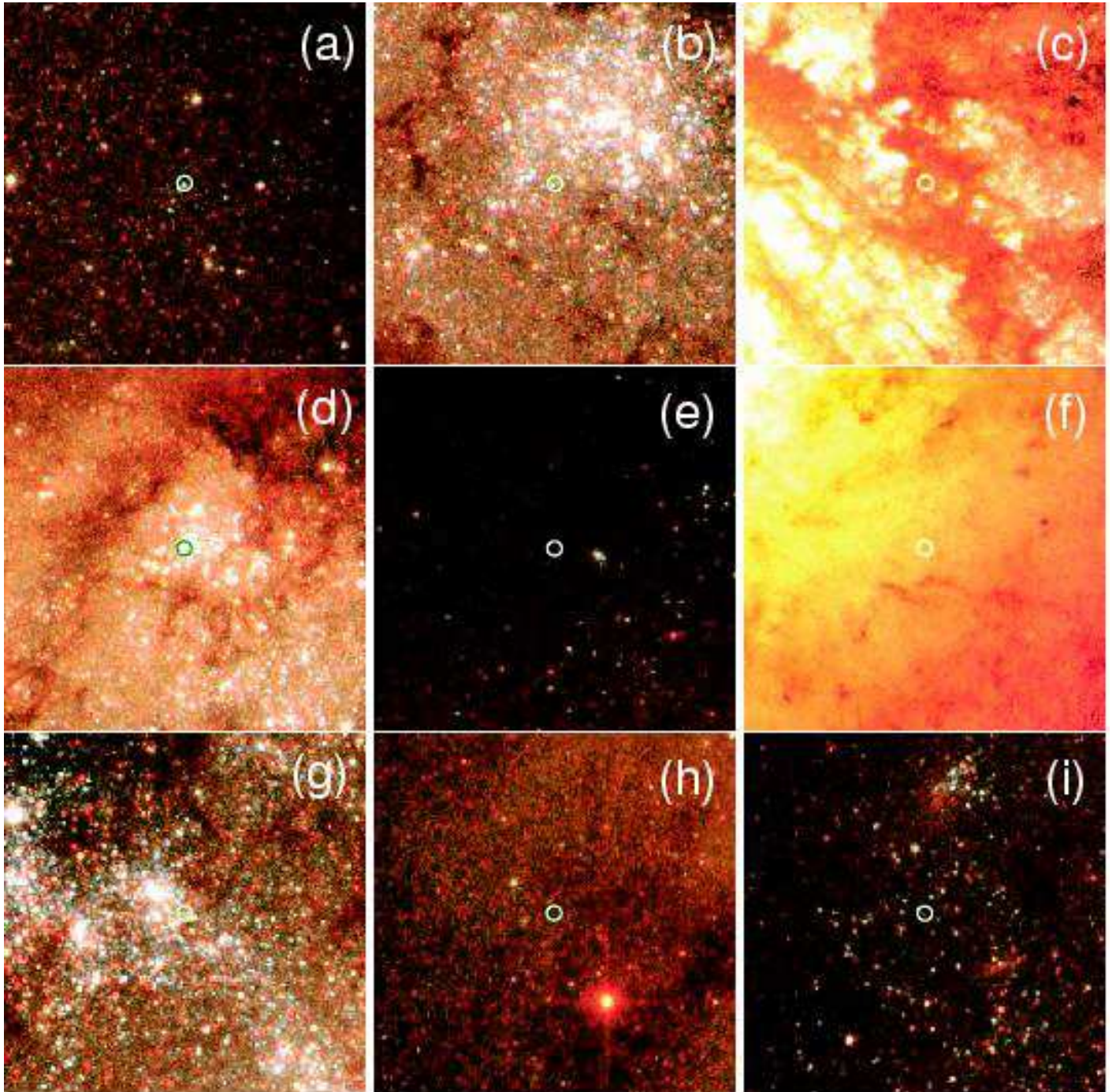


FIG. 1.— ACS true-color images around the nine ULXs in M51. Red, green, and blue correspond to the F435W, F555W, and F814W filters, respectively. The adopted error circles of ULXs, with a  $0.3''$  radius, is shown. The size of each image is  $15'' \times 15''$  or  $610 \text{ pc} \times 610 \text{ pc}$ . North is up and east is to the left. Fig 1a–1i correspond to ULX-1 to ULX-9, respectively.

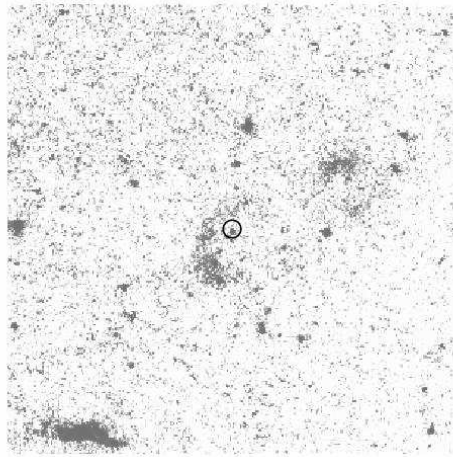


FIG. 2.— ACS F658N ( $H\alpha$ ) images around ULX-1. Image size is same as Fig. 1. North is up and east is to the left.



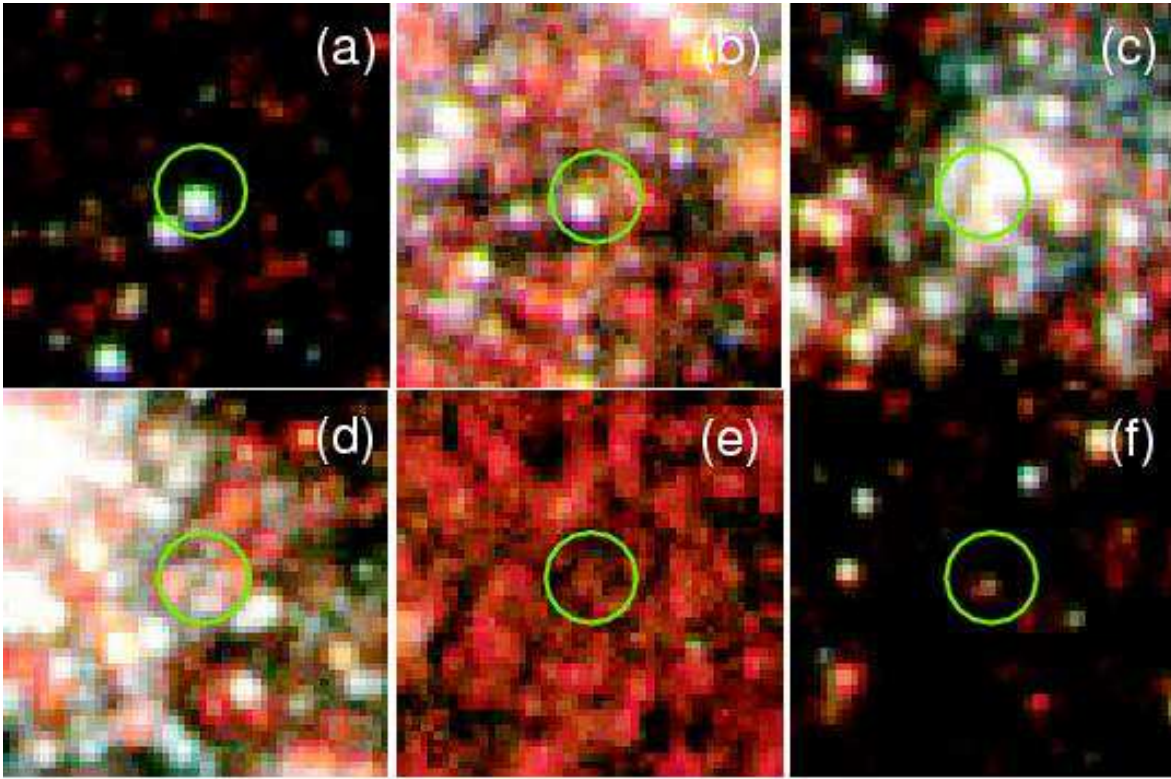


FIG. 3.— ACS true-color images of the  $2.5'' \times 2.5''$  region around the ULXs with possible counterparts. The colors and error circle are same as Fig. 1. Fig 3a–3f correspond to ULX-1, 2, 4, 7, 8, and 9, respectively.

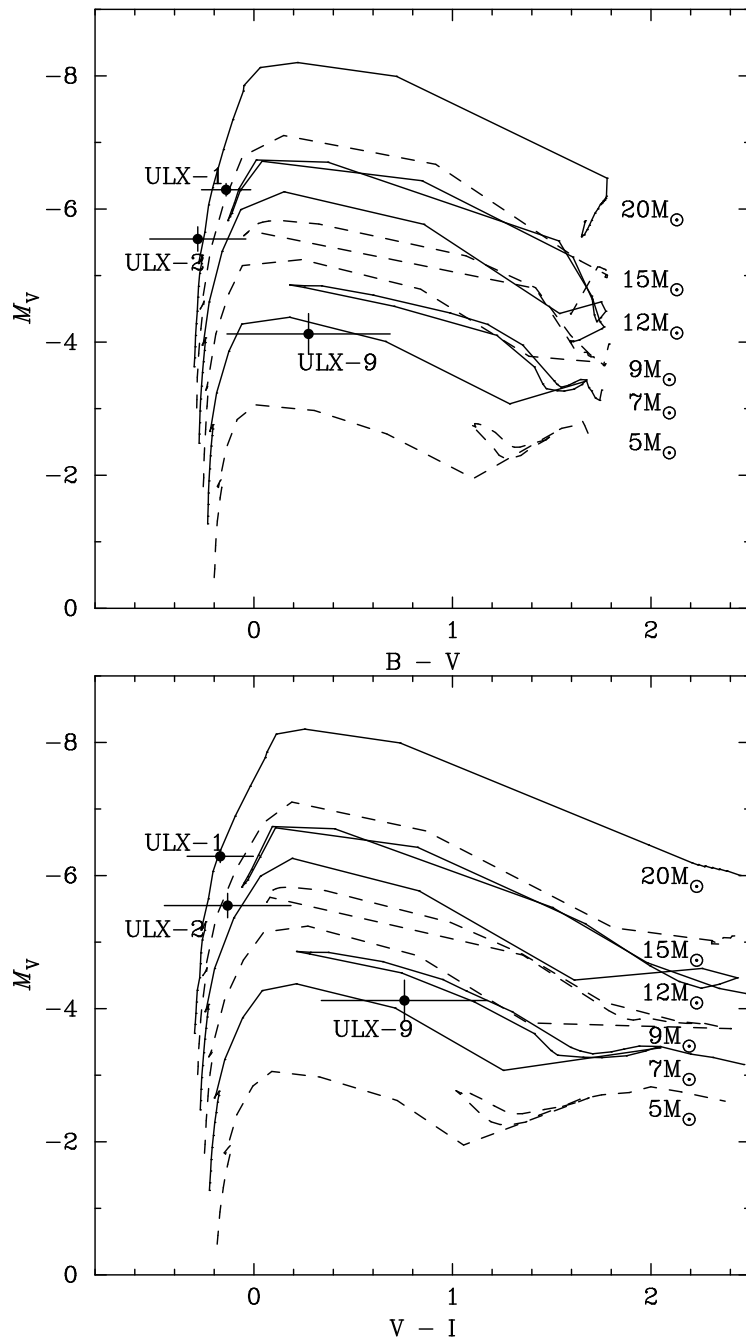


FIG. 4.— Locations of candidate counterparts of ULX-1, ULX-2, and ULX-9 in color-magnitude diagrams. The stellar evolutionary tracks of  $20M_{\odot}$ ,  $15M_{\odot}$ ,  $12M_{\odot}$ ,  $9M_{\odot}$ , and  $7M_{\odot}$  (from top to bottom) of Lejeune & Scherer (2001) are shown as solid and dashed lines.